Simulation, Fabrication and Characterization of an Integrated Plasmonic Polarizer on Ti Diffused LiNbO3 Channel Waveguide

Keyvan Ahmadi (keyvanah@shirazu.ac.ir)
Shiraz University Faculty of Sciences https://orcid.org/0000-0001-8123-2839
Mohamad Hossein Poorghadiri Isfahani
Shahid Beheshti University
Mohamad Hossein Fathi
Shiraz University

Research Article

Keywords: Integrated polarizer, Plasmonic, LiNbO3, Ti channel waveguide, Extinction ratio, Insertion loss

Posted Date: March 22nd, 2021

DOI: https://doi.org/10.21203/rs.3.rs-300448/v1

Simulation, fabrication and characterization of an integrated plasmonic polarizer on Ti diffused $LiNbO_3$ channel waveguide

Keyvan. Ahmadi[11]*, Mohamad.Hossein. Poorghadiri Isfahani[2], Mohamad.Hossein. Fathi[1]

[1]Department of Physics, College of Science, Shiraz University, Shiraz, Fars, 71946-24795, Iran

[1]Department of Electrical Engineering, College of Engineering, Shiraz University, Shiraz, Fars, 71946-24795, Iran

[2]Laser & Plasma Research Institute, Shahid Beheshti University, Evin, Tehran 1983963113, Iran

Abstract- In this work the design, fabrication and characterization of a TE-pass plasmonic waveguide polarizer on Ti in-diffused channel waveguide fabricated on x-cut $LiNbO_3$ substrate are reported. By deposition of MgF_2 of 5nm thickness as the buffer layer and Au layer of about 30nm thickness as the cladding layer the polarization extinction ratio was measured to be 32dB and insertion loss for TE mode was about 2dB in a single mode channel waveguide of 2.1cm length.

Keywords: Integrated polarizer, Plasmonic, $LiNbO_3$, Ti channel waveguide, Extinction ratio, Insertion loss

Introduction

An optical waveguide polarizer is an essential component in Ti in-diffused $LiNbO_3$ integrated circuits to obtain acceptable performance. Switching networks, high dynamic range intensity modulators and optical fiber gyro circuits require the optical source to be linearly polarized and confined to one of the orthogonal modes. Optical power of the unwanted polarization state would degrade the performance of the aforementioned circuits by increasing crosstalk, reducing the dynamic range and bias drift respectively. For better reliability and lower cost advanced optical devices such as interferometric fiber optic gyros require the integration of both passive and active functions on the same substrate. As we know $LiNbO_3$ waveguide devices have been widely used because of their excellent electro-optic, acousto-optic and nonlinear properties.

Various solutions proposed for making such polarizers include (1) use of an anisotropic leaky wave polarizer in an anisotropic crystal such as $LiNbO_3$ (2) propagation in a direction oblique to the optic axis to make one of the modes leaky and (3) metal cladding to introduce differential losses between TE and TM modes. Extinction ratio of 32dB/cm and insertion loss of 0.9dB/cm have been reported on the y-cut $LiNbO_3$ substrate at 1.55µm benefiting from process-dependence characteristics of TE-pass Zn-diffused waveguides [1-6]. Of the proposed solutions, the metal-cladded polarizer is the most interesting since it is integrable with the optical circuit and is expected to reach a high differential attenuation polarization. Ordinary polarizers based on dielectric structures require large device length to accumulate enough polarization effect due to weak birefringence which inhibits their integration with other optical devices. On the contrary, hybrid plasmonic waveguide and hybrid plasmonic grating are very compact and only several microns. Multilayer metal clad waveguides with a low index buffer layer can be designed as a highly efficient polarizer if various layer thicknesses are appropriately optimized. The polarizer is based on the resonant coupling of guided modes to the surface plasmon mode supported by the metal. In general metal clad optical waveguides are suitable for electro-optic, magneto-optic devices and mode filters. It is well known that the ohmic losses of a TM guided mode are much larger than that of a TE mode at optical wavelengths. Mode filters are designed to utilize the larger TM to TE loss ratio in a metalized planar dielectric waveguide structure. To reduce the insertion

[1] Keyvan Ahmadi

keyvanah@shirazu.ac.ir

losses of waveguide devices with metal cladding, a dielectric layer (buffer layer) of lower refractive index is inserted between the waveguide and the metal. For TM mode there is a resonant absorption peak at a certain critical value of the buffer layer thickness, which results from a guided mode to the lossy surface-plasmon mode supported by the metal. A good polarizer must have a high extinction ratio without introducing a significant loss in the transmitted light (TE mode). However, hybrid plasmonic polarizers suffer from thermal instability induced by heat converted from TM mode. Another much more practical structure is hybrid plasmonic grating which reflects TE/TM mode based on theory of bragg grating with both index and mode overlap taken into consideration. More research are carrying out on Lithium Niobate on Insulator (LNOI) platform due to its excellent electro-optic and remarkable birefringence and large optical nonlinearity [7]. In LNOI platform, shallowly etch ridge waveguide polarizer with 25dB extinction ration in 1mm and a hybrid plasmonic grating with 20dB extinction ration and 2.5dB insertion loss in a length of only 23µm are reported [8]. A compact TM-pass polarizer using hybrid plasmonic grating structure with ER as high as 20dB and insertion loss less than 2.5dB has been recently reported on LNOI platforms [9].

In this work we started with numerical simulations of a waveguide plasmonic polarizer on Ti in-diffused $LiNbO_3$ channel waveguide for MgF_2 as buffer and Au, Ag and Al as metallic overlays. The buffer layer (MgF_2) thickness was taken at its critical value for Au metal then its thickness was also optimized. Finally, we fabricated and characterized the device with the combination of MgF_2 and Au since it promised good performance and ease of fabrication.

Simulation results

To achieve highly polarizing waveguides the anisotropy-based polarization waveguiding of the Ti in-diffused channel waveguides are of advantageous. The increment of the refractive indices of the TE and TM mode, which affects the confinement of the desired mode, are governed by the four parameters of the thermal diffusion process: Ti waveguide strip, Ti coating thickness, diffusion temperature and diffusion duration. It is found that the refractive index anisotropy is high for Ti width 8µm, thickness 100 nm, temperature 1060 °C and duration 10h. The channel waveguide simulated under these parameters on $LiNbO_3$ operates in a single mode regime for 1550 nm. Single mode guiding helps avoid various mode dispersion and intermodal interference effects and is therefore preferred in integrated photonics. Mode intensity profiles for TE and TM mode at 1550 nm wavelength simulated by COMSOL 5.4 have been shown in Fig.1. The light intensity of the TM and TE guided modes follows a Gaussian function $A_x exp(-2(x/W_x)^2)$ in the width direction x and a Hermite-Gaussian function $A_y y^2 exp\left(-2(y/W_y)^2\right)$ in the depth direction y. The modes under two polarizations have sizes of $W_x * W_y$ =6.4*9 µm^2 for the TE mode and 8.1*9.96 µm^2 for the TM mode. It is evident that fundamental TM mode is less confined compared to TE mode for Ti in-diffused waveguide on x-cut $LiNbO_3$ substrate and this considered advantageous in designing more efficient waveguide polarizers.

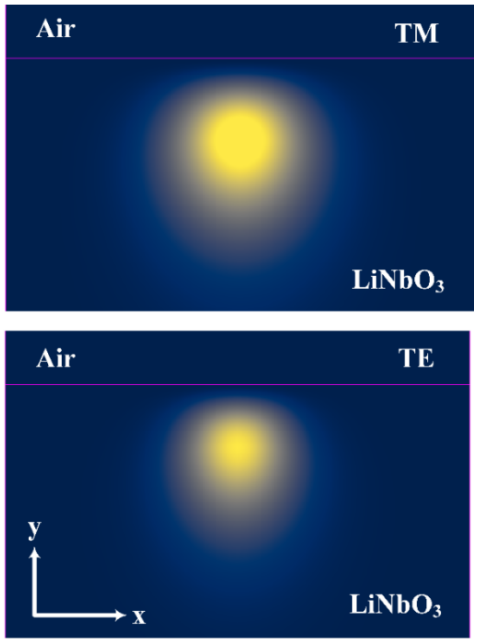

Fig.1 TM and TE mode light intensity profiles along width x and depth y directions of 8µm-wide Ti: $LiNbO_3$

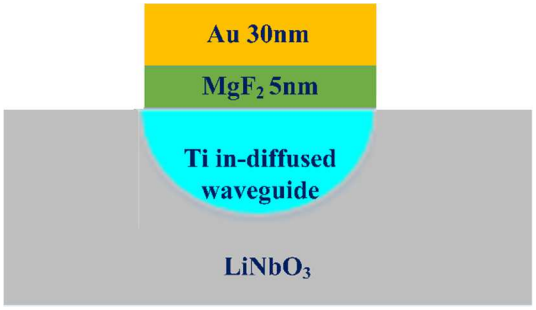

Fig. 2 Cross-section schematic of a TE pass plasmonic polarizer on Ti in-diffused channel waveguide

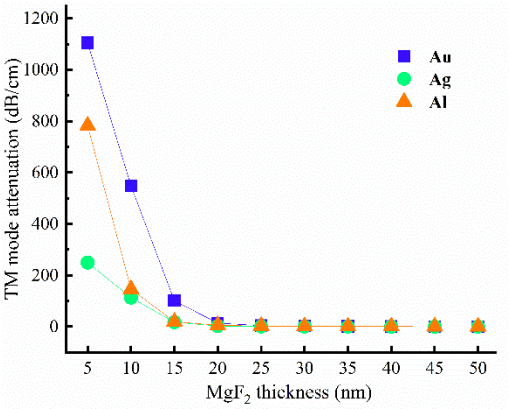

Fig.3 Variation of the TM mode light attenuation with buffer layer (MgF_2) thickness for Ag, Au and Al as metal layers

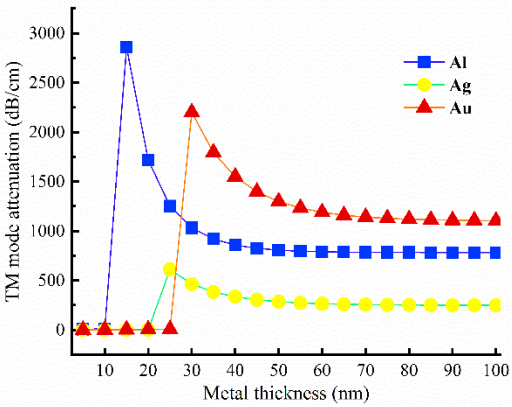

Fig.5 Variation of the TM mode light attenuation with metal thicknesses of Ag, Au and Al at critical buffer MgF_2 thickness 5nm

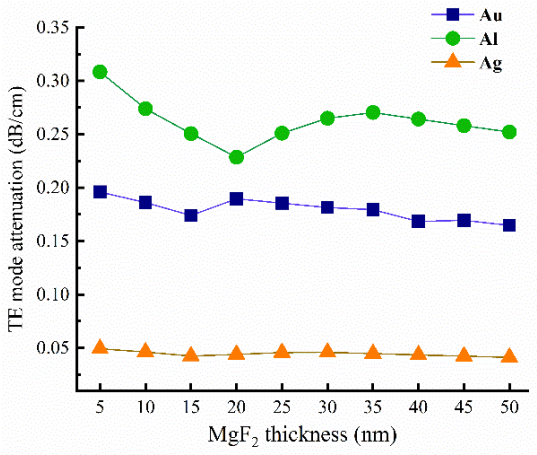

Fig.4 Variation of the TE mode light attenuation with buffer layer (MgF_2) thickness for Ag, Au and Al as metal layers

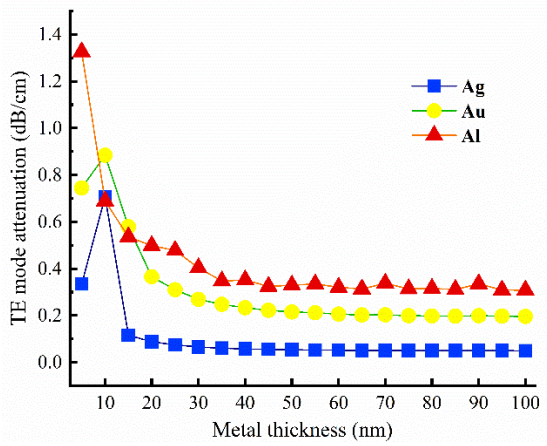

Fig.6 Variation of the TE mode light attenuation with metal thicknesses of Ag, Au and Al at critical buffer MgF_2 thickness 5nm

Fig.2 shows the schematic configuration of the proposed polarizer, which is composed of Ti in-diffused channel waveguide with a layer of MgF_2 (buffer layer) and Au on top of it.

A: Polarizer with varying buffer thickness

Here we will begin with a discussion of the 2D finite element methods of COMSOL 5 used to design the polarizer and study its characteristics. The operation wavelength is 1.55µm, which is matched to the standard SMF-28 type optical fiber. The corresponding refractive indices for Au, Ag, Al, and MgF_2 are 0.52+10.7, 0.14+11.36, 1.128+15.49 and 1.37 respectively. Fig.3 shows the dependence of the TM mode attenuation on the buffer layer thickness with taking metal thickness 100nm (semi-infinite). There is a resonant absorption for TM mode at buffer thickness lass than 5nm and then it starts to decrease significantly. Au and Al show stronger absorption than Ag layer at 5nm thickness. The peak absorption loss is caused by the TM mode coupling to a lossy surface plasmon mode bound to buffer/metal interface. Fig.4 show the variation of the TE mode as a function of buffer layer for metals Au, Ag and Al at 100nm thickness. The TE mode attenuation at critical value for Au, Ag and Al is 0.2dB/cm, 0.31dB/cm and 0.05dB/cm respectively. It is also observed that the attenuation coefficient of the TE modes decreases with increase in buffer thickness due to the relaxation of the metal's influence on the guided modes by the thicker buffer layer.

B: Polarizer with varying metal thickness

Let us consider the effect of metal thickness at critical value of the MgF_2 buffer thickness (5 nm) on TM and TE mode attenuation ratio. As evident from figs 3 and

4 the ratio of TM to TE absorption losses at critical value of 5nm is large that can be increased further by taking the metal thickness into consideration. At the critical buffer thickness, the metal thickness is varied from 5 to 100nm. The attenuation of the TM mode reached maximum at certain particular metal thicknesses. It is observed that the attenuation starts to decrease and then reaches a constant value as shown in Fig.5. The metal thickness of the maximum attenuation for TM mode is 30, 25 and 15nm for Au, Ag and Al. The enhanced attenuation for thin metal films is due to the coupling between the surface plasmon wave associated with each boundary (buffer and air). It is observed in Fig.6 that the TE loss at critical values for Au, Ag and Al where the MgF_2 is 5nm is nearly 0.3, 0.10 and 0.5dB/cm respectively. Fig.7 shows the filed distribution of TM and TE modes for a buffer layer of 5nm and Au film of 30nm. It is also observed the composition of the TM mode and the surface plasmon mode which results in high absorption loss whereas there is no coupling for guided TE mode and surface plasmon mode.

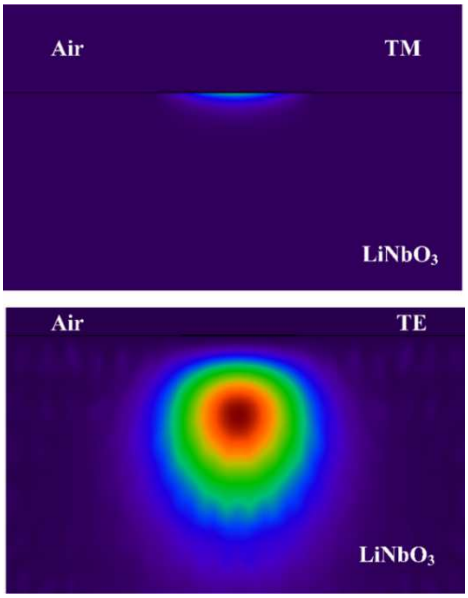

Fig.7 TM and TE mode profiles with a buffer layer of 5nm and Au layer of 30nm thickness.

Fabrication and characterization

Then we proceeded with the fabrication of a Ti in-diffused channel waveguide polarizer on the x-cut $LiNbO_3$ substrate. The required steps for fabrication of a Ti channel waveguide are photolithography and wet etching for creating strips on LN, deposition of Ti layer and lift-off technique, and Ti diffusion processes at high temperatures. In the photolithography step, we used AZ5214E positive-tone photoresist to facilitate the lift-off process. After photolithography, Ti layer of 100nm thickness with the rate of 1nm/sec and $1e^{-7}$mba*r* pressure was deposited with the E-gun evaporator followed by the lift-off process. In this step, we immersed the sample in a bath of 1-Methyl-2-Pyrrolidone (NMP) to remove the residual Ti layer so that Ti strips of 8µm width on our sample were delineated. The strips orient along the y-axis of the crystal. The Ti in-diffusion was performed at 1060°C for 10h in an environment of following O_2 bubbled through room-temperature water at a rate of 1lit/min. Finally, the waveguide end facets of the samples was optically polished with a polishing machine (Ultratec company) to reduce the butt-coupling loss in our experiment. After fabrication and polishing the sample a thin layer of MgF_2 (5nm thickness) was deposited on top of Ti channel waveguide and finally a layer of 30nm Au was deposited on MgF_2 layer with a magnetron sputtering. Fig.8 shows the whole process of the polarizer fabrication. A SEM image of the fabricated polarizer has also been presented in Fig.8. The MgF_2 layer of 5nm thickness is not observed in the SEM image and not indicated in the Fig.8.

Then we proceeded with the characterization of the fabricated device by using an end-fire scheme to test the fabricated device. In the experimental setup, light from a CW laser operating in 1550 nm wavelength was coupled to the endface of the waveguide. To ensure coupling in and out of the waveguide a coupler 50/50 was used to combine the signal laser at 1550 nm and a laser diode at 980 nm. After coupling 1550 nm with the help of 3-axis positioning stage of 1µm resolution (Thorlabs company) the output power was recorded with a high accuracy extinction ratio meter of 0.5dB (ERM100,Thorlabs). The coupling setup was shown in the Fig.9. The output laser spot at 980 nm recorded with the visible camera of 500× magnification is seen. For the 2.1cm length the observed extinction ratio was 32dB (about 1000:1) and the insertion loss was measured to be 2dB for TE mode. The insertion loss for TE mode at 1550nm wavelength includes the mismatch profile loss between fiber and waveguide facetes, the Fresnel loss, the scattering loss and ohmic absorption loss. The mismatch profile loss was estimated to be 0.3dB/facet while the minimum Fresnel reflection loss between the waveguide and the SMF-28 fiber endfacet is taken to be 0.15dB/facet (total reflection loss is 0.3dB). The ohmic loss at 5nm MgF_2 and 30nm Au layer was 0.63dB.

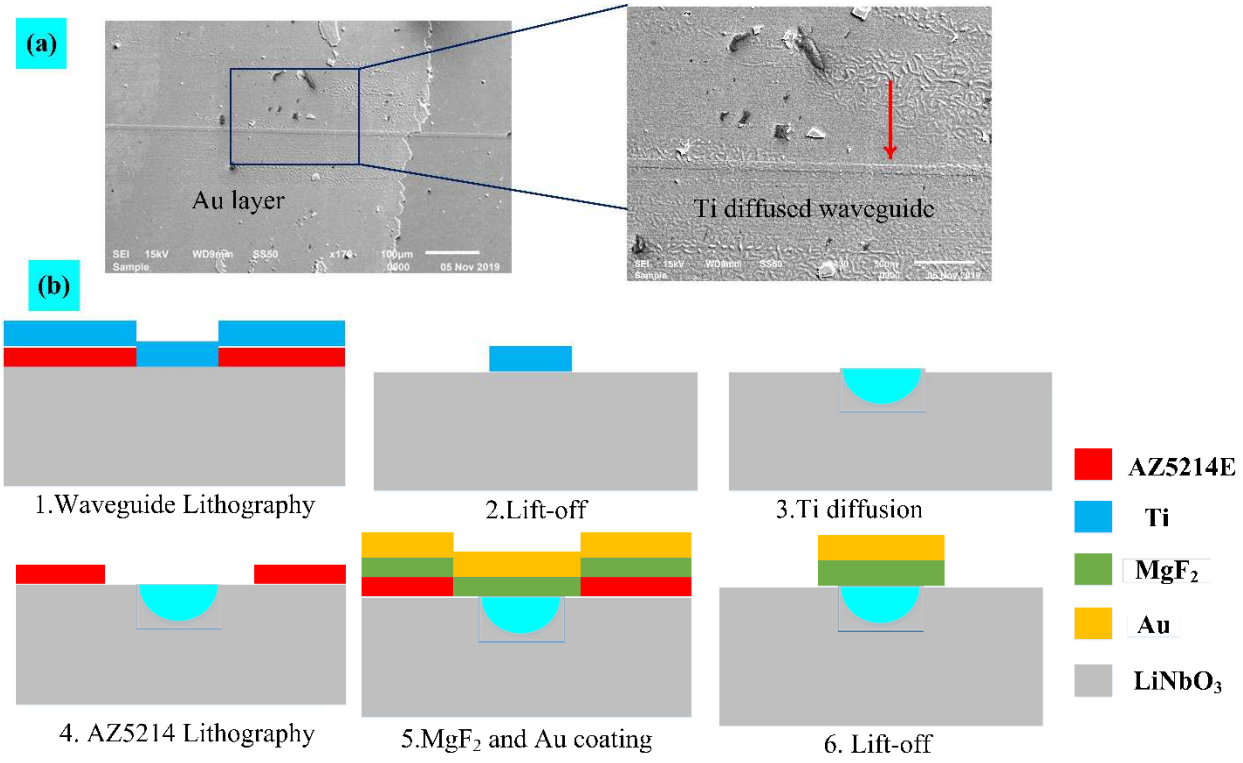

Fig.8 (a) SEM image of the fabricated plasmonic polarizer on a 8μm-width Ti: $LiNbO_3$ channel waveguide. MgF_2 layer of 5nm thickness is not clear.(b) The schematic diagram of the polarizer fabrication process

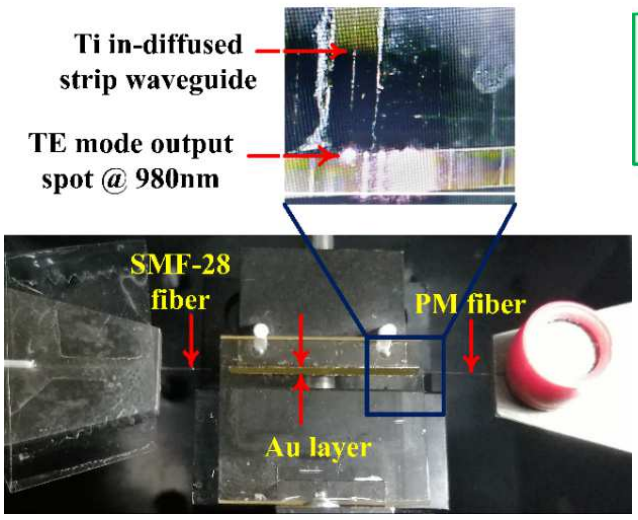

Fig.9 Coupling setup for characterization of the plasmonic polarizer.

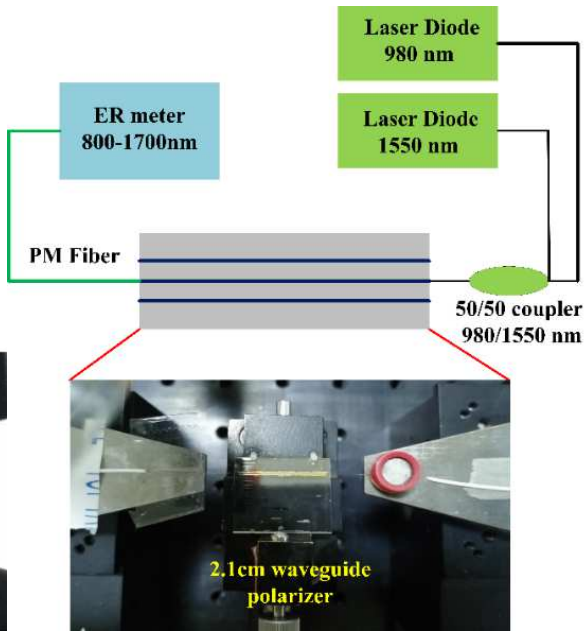

Fig.10 Characterization setup of the plasmonic polarizer.

Results and discussion

Table 1. Data reported on integrated polarizers in recent years

Year	WG material	Wavelength(nm)	Mechanism	ER(dB)	References
2019	SU-8	1510	Birefringence	14	[15]
2012	Silicon	1550	Plasmonic	15	[19]
2010	GaAs-InP	1550	Photnic crystal	16	[20]
2012	Resin Polymer	1310	Absorbance	19	[18]
1997	Polymer	1550	Birefringence	21	[16]
2008	Silicon	1315	Plasmonic	30	[11]
2019	Germanium	1540	Grating	30	[13]
2006	$LiNbO_3$	1550	Plasmonic	32	[1]
1998	Silica	1310	Birefringence	39	[17]
2014	Silicon	1550	Grating	40	[14]
1982	K-Na	836	Plasmonic	43	[10]
1999	PMMA	820	Metal grating	50	[12]

The result of 32dB for extinction ratio differs from simulation results at critical value for MgF_2 and Au layer which could be attributed mainly to variation in MgF_2 thickness and its refractive index due to humidity absorption. Table.1 shows the ER value for integrated polarizers reported in the literatures for comparison.

Conclusion

A low loss, integrated TE pass polarizer using hybrid plasmonic waveguide is demonstrated in $LiNbO_3$ substrate, which provide a more compact, and efficient photonics element in combination with a phase modulator y-branch waveguide in IFOG sensors. With adjusting the thickness of MgF_2 (buffer) and Au (clad) a high extinction ratio of 32dB and low insertion loss of 2dB was measured for the fabricated device. The 1310 and 980 nm wavelengths used in fiber optic gyro sensors were not investigated in this work since the fabricated waveguides on $LiNbO_3$ does not operate in a single mode regime.A critical limitation in the selection of a metal for a stable polarizer is that the metal surface exposed to atmosphere must be pure. Oxides and other films formed by atmospheric exposure may change the resonant coupling condition between the guided mode and surface plasmon polaritons. Use of Ag as a cladding layer has one disadvantage, as it is highly susceptible to oxidation. Therefore Ag may not be a good choice for cladding layer. We chose Au since it was very resistant to oxidation and other contaminants.

Funding

Not applicable

Conflicts of interest/Competing interests

Not applicable

Availability of data and material

Not applicable

Code availability

Not applicable

Authors' contributions

Not applicable

Ethics approval

Not applicable

Consent to participate

Not applicable

Consent for publication

Not applicable

Reference

[1] Twu, R.C., Huang, C.C. and Wang, W.S., (2006). TE-pass Zn-diffused $LiNbO_3$ waveguide polarizer. *Microwave and Optical Technology Letters*, *48*(11), pp.2312-2314.

[2] Masuda, M. and Koyama, J., (1977). Effects of a buffer layer on TM modes in a metal-clad optical waveguide using Ti-diffused $LiNbO_3$ C-plate. *Applied optics*, *16*(11), pp.2994-3000.

[3] Dobrusin, V. and Ruschin, S., (2008). Fabrication of integrated Ti: $LiNbO_3$ waveguide polarizer. *Optical Engineering*, *47*(12), p.120504.

[4] Henning, H.J., (1986). Thin-film polariser for Ti: $LiNbO_3$ waveguides at 1.3μm. *Electronics Letters*, *14*(22), pp.756-757.

[5] Il'ichev, I.V., Toguzov, N.V. and Shamray, A.V., (2009). Plasmon-polariton polarizers on the surface of single-mode channel optical waveguides in lithium niobate. *Technical Physics Letters*, *35*(9), p.831.

[6] Thyagarajan, K., Bourbin, Y., Enard, A., Vatoux, S. and Papuchon, M., (1985). Experimental demonstration of TM mode-attenuation resonance in planar metal-clad optical waveguides. *Optics letters*, *10*(6), pp.288-290.

[7] Shi, J., Chen, X., Xia, Y. and Chen, Y., (2003). Polarization control by use of the electro-optic effect in periodically poled lithium niobate. *Applied optics*, *42*(28), pp.5722-5725.

[8] Saitoh, E., Kawaguchi, Y., Saitoh, K. and Koshiba, M., (2013). TE/TM-pass polarizer based on lithium niobate on insulator ridge waveguide. *IEEE Photonics Journal*, *5*(2), pp.6600610-6600610.

[9] Yu, W., Dai, S., Zhao, Q., Li, J. and Liu, J., (2019). Wideband and compact TM-pass polarizer based on hybrid plasmonic grating in LNOI. *Optics Express*, *27*(24), pp.34857-34863.

[10] Bloemer, M.J. and Haus, J.W., (1992). Compact, high-extinction waveguide polarizers that use localized surface plasmons. *Optics letters*, *17*(8), pp.598-600.

[11] Avrutsky, I., (2008). Integrated optical polarizer for silicon-on-insulator waveguides using evanescent wave coupling to gap plasmon–polaritons. IEEE Journal of selected topics in quantum electronics, 14(6), pp.1509-1514.

[12] Wang, J., Schablitsky, S., Yu, Z., Wu, W. and Chou, S.Y., (1999). Fabrication of a new broadband waveguide polarizer with a double-layer 190 nm period metal-gratings using nanoimprint lithography. *Journal of Vacuum Science & Technology B: Microelectronics and Nanometer Structures Processing, Measurement, and Phenomena*, *17*(6), pp.2957-2960.

[13] Posner, M.T., Podoliak, N., Smith, D.H., Mennea, P.L., Horak, P., Gawith, C.B., Smith, P.G. and Gates, J.C., (2019). Integrated polarizer based on 45° tilted gratings. *Optics express*, *27*(8), pp.11174-11181.

[14] Guan, X., Chen, P., Chen, S., Xu, P., Shi, Y. and Dai, D., (2014). Low-loss ultracompact transverse-magnetic-pass polarizer with a silicon subwavelength grating waveguide. *Optics letters*, *39*(15), pp.4514-4517.

[15] Berahim, N., Amiri, I.S., Anwar, T., Azzuhri, S.R., Nasir, M.M., Zakaria, R., Chong, W.Y., Lai, C.K., Lee, S.H., Ahmad, H. and Ismail, M.A., (2019). Polarizing effect of MoSe2-coated optical waveguides. *Results in Physics*, *12*, pp.7-11.

[16] Lee, S.S., Ahn, S.W. and Shin, S.Y., (1997). Integrated optical waveguide polarizer based on photobleaching-induced birefringence in an electrooptic polymer. *IEEE Photonics Technology Letters*, *9*(8), pp.1125-1127.

[17] Morand, A., Sanchez-Perez, C., Benech, P., Tedjini, S. and Bose, D., (1998). Integrated optical waveguide polarizer on glass with a birefringent polymer overlay. *IEEE Photonics Technology Letters*, *10*(11), pp.1599-1601.

[18] Kim, J.T. and Choi, C.G., (2012). Graphene-based polymer waveguide polarizer. *Optics express*, *20*(4), pp.3556-3562.

[19] Bhatt, G.R. and Das, B.K., (2012). Improvement of polarization extinction in silicon waveguide devices. *Optics Communications*, *285*(8), pp.2067-2070.

[20] Ma, P., Strasser, P., Kaspar, P. and Jackel, H., (2010). Compact and integrated TM-pass photonic crystal waveguide polarizer in InGaAsP–InP. *IEEE Photonics Technology Letters*, *22*(24), pp.1808-1810.

Figures

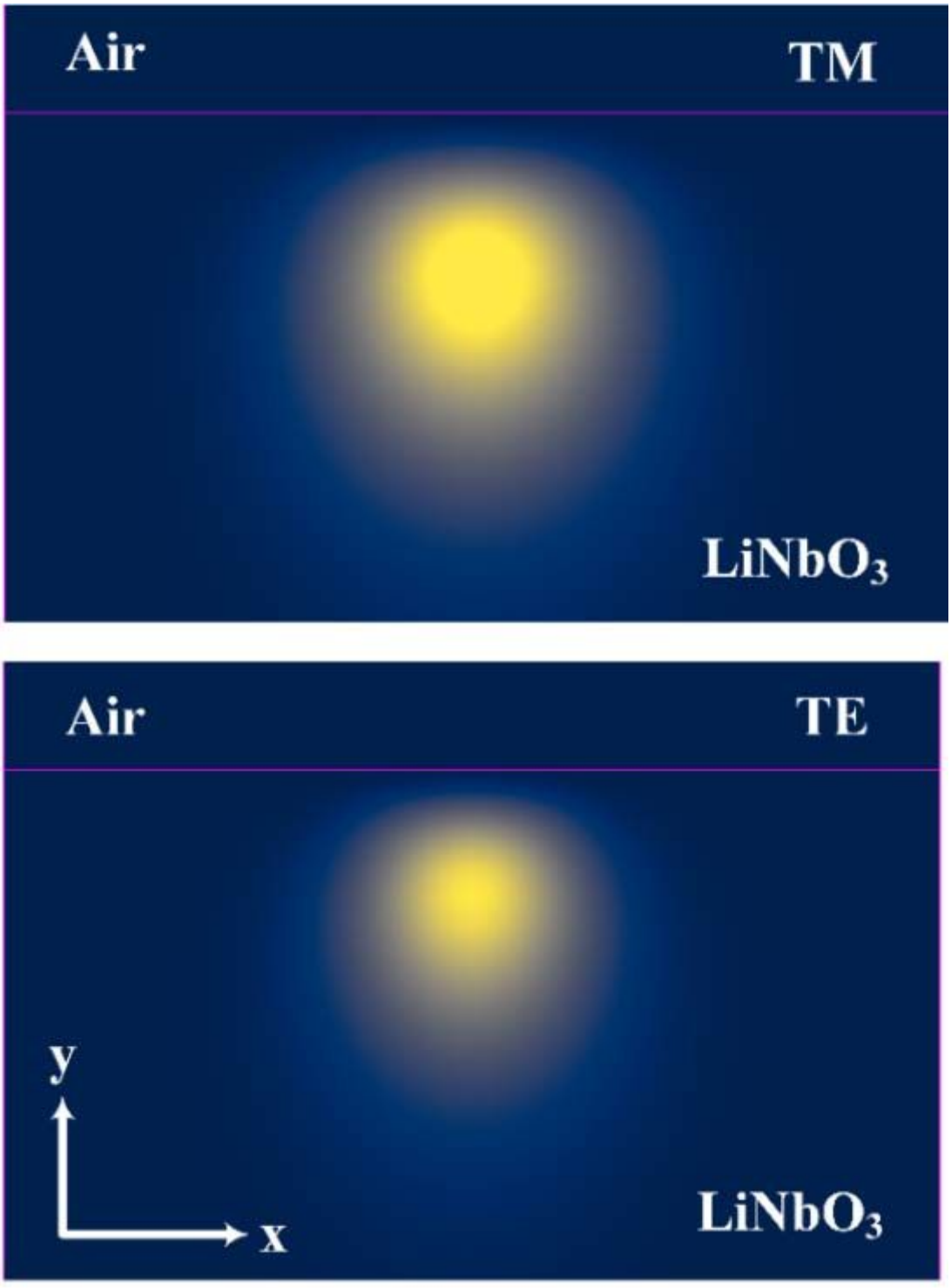

Figure 1

TM and TE mode light intensity profiles along width x and depth y directions of 8μm-wide Ti: LiNbO3

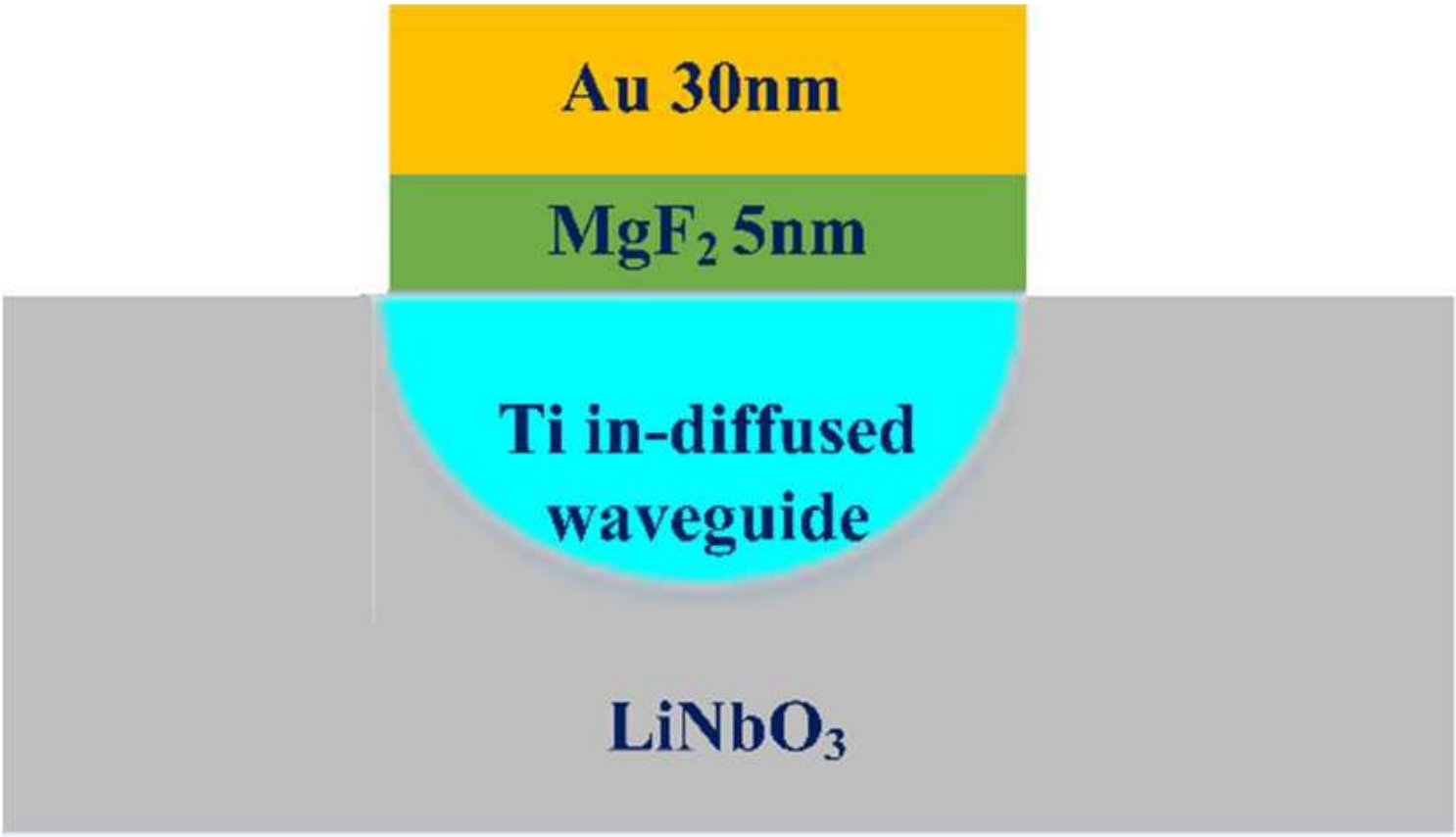

Figure 2

Cross-section schematic of a TE pass plasmonic polarizer on Ti in-diffused channel waveguide

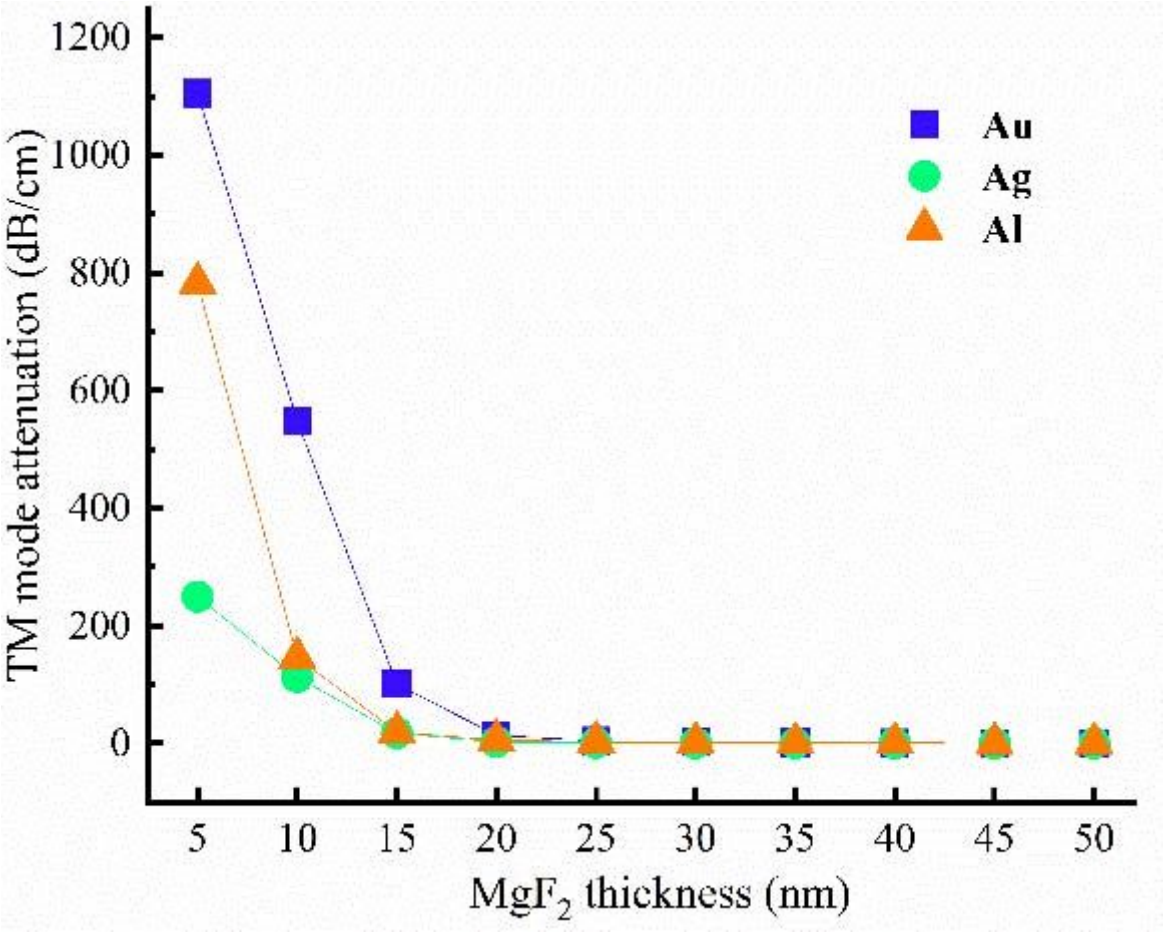

Figure 3

Variation of the TM mode light attenuation with buffer layer (MgF2) thickness for Ag, Au and Al as metal layers

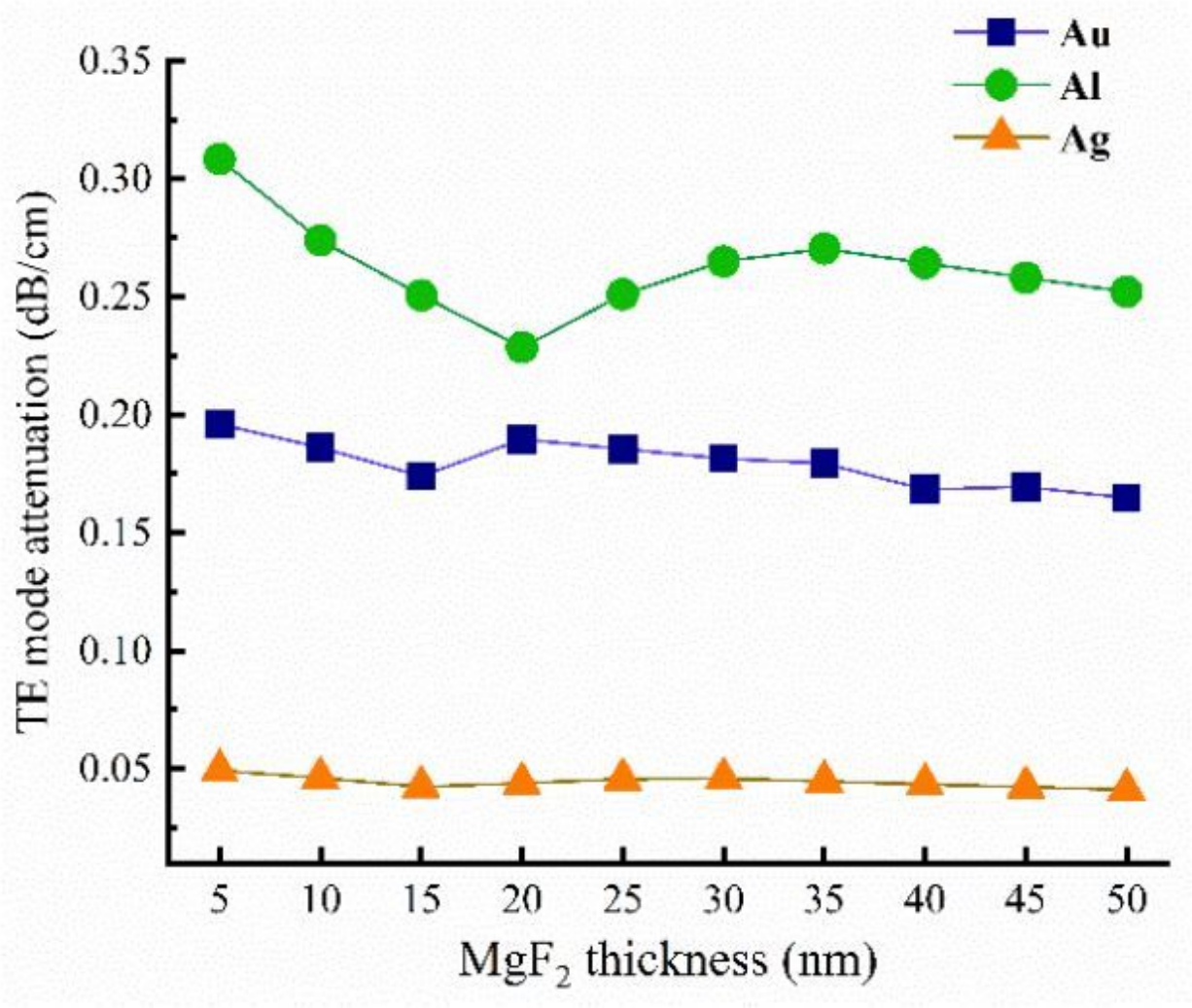

Figure 4

Variation of the TE mode light attenuation with buffer layer (MgF2) thickness for Ag, Au and Al as metal layers

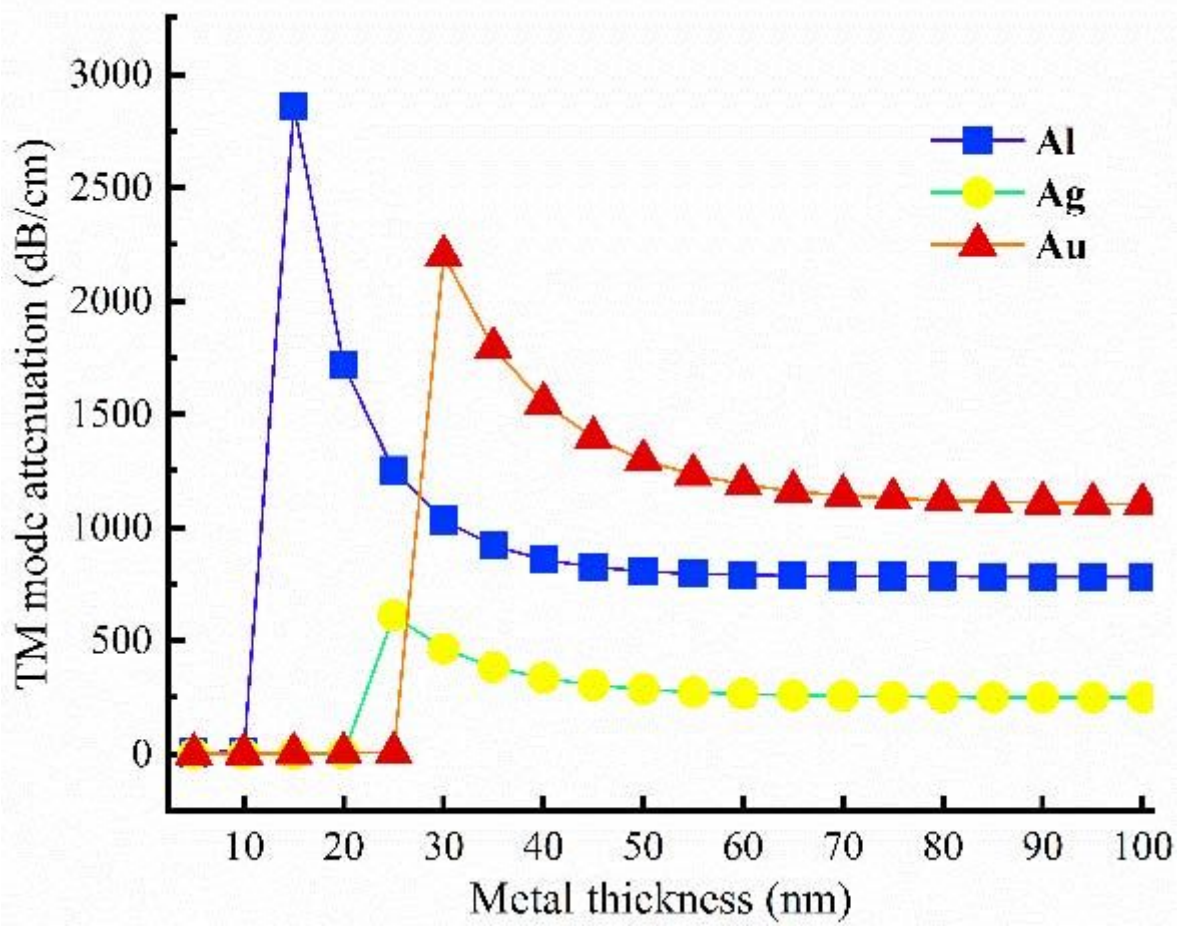

Figure 5

Variation of the TM mode light attenuation with metal thicknesses of Ag, Au and Al at critical buffer MgF2 thickness 5nm

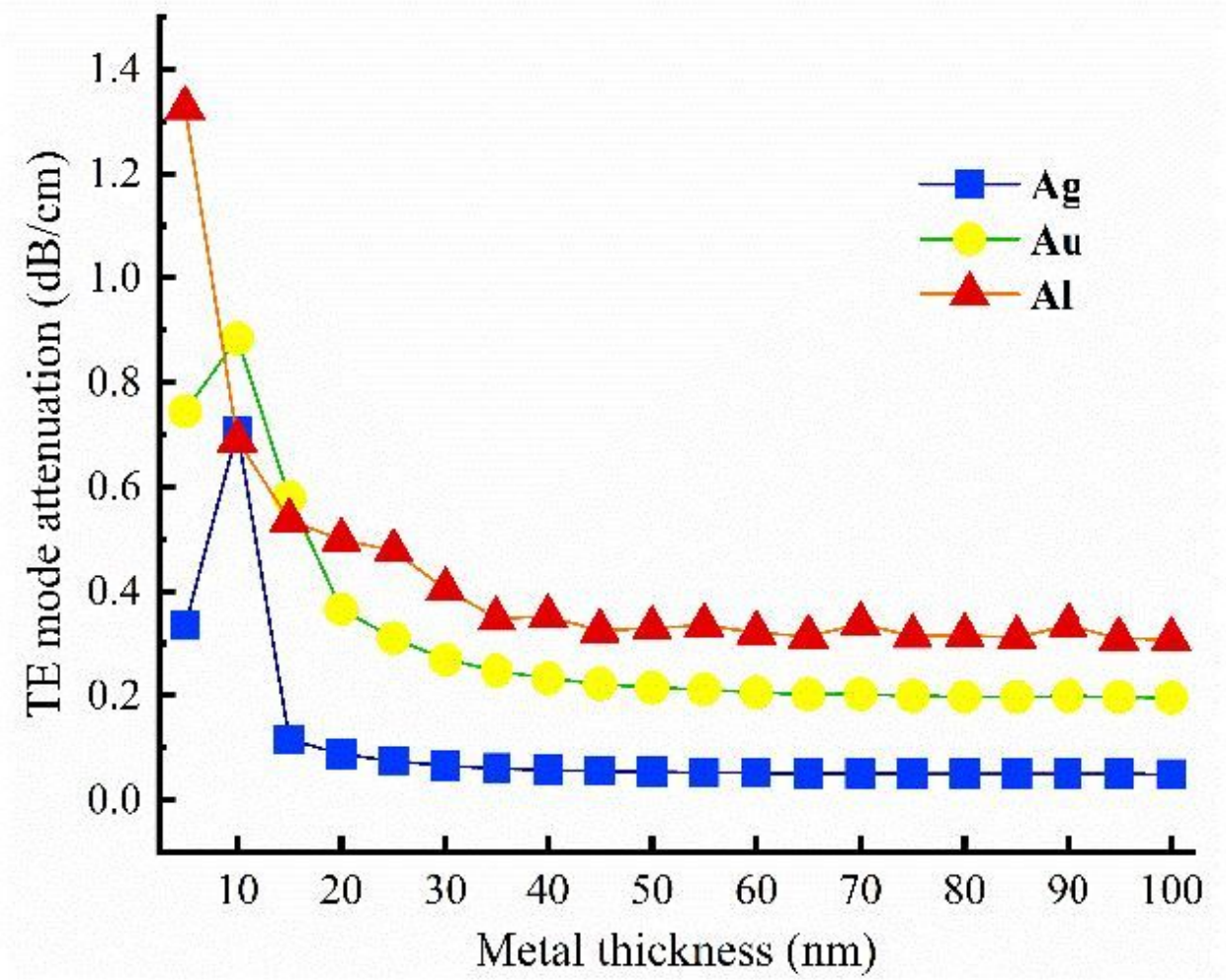

Figure 6

Variation of the TE mode light attenuation with metal thicknesses of Ag, Au and Al at critical buffer MgF2 thickness 5nm

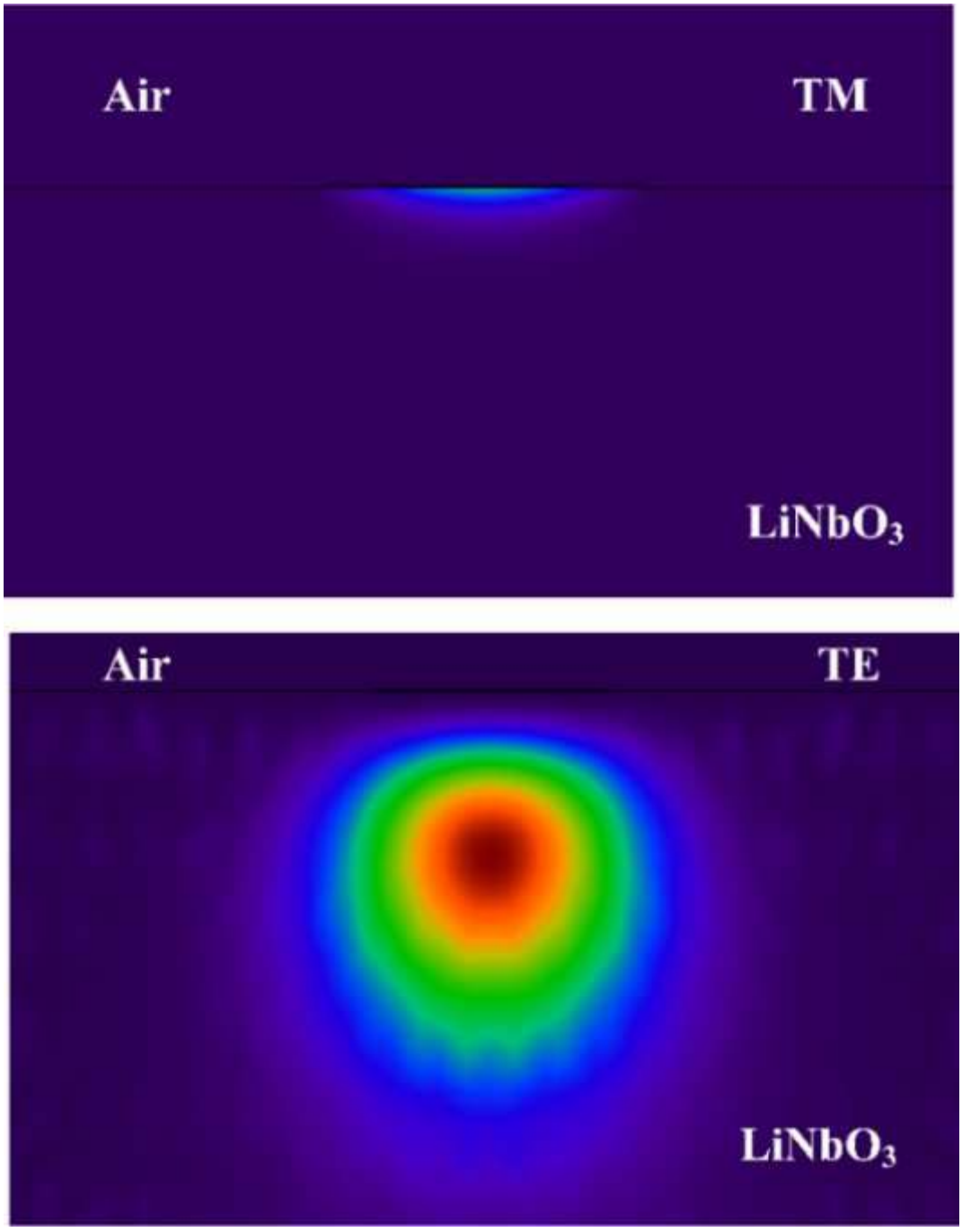

Figure 7

TM and TE mode profiles with a buffer layer of 5nm and Au layer of 30nm thickness.

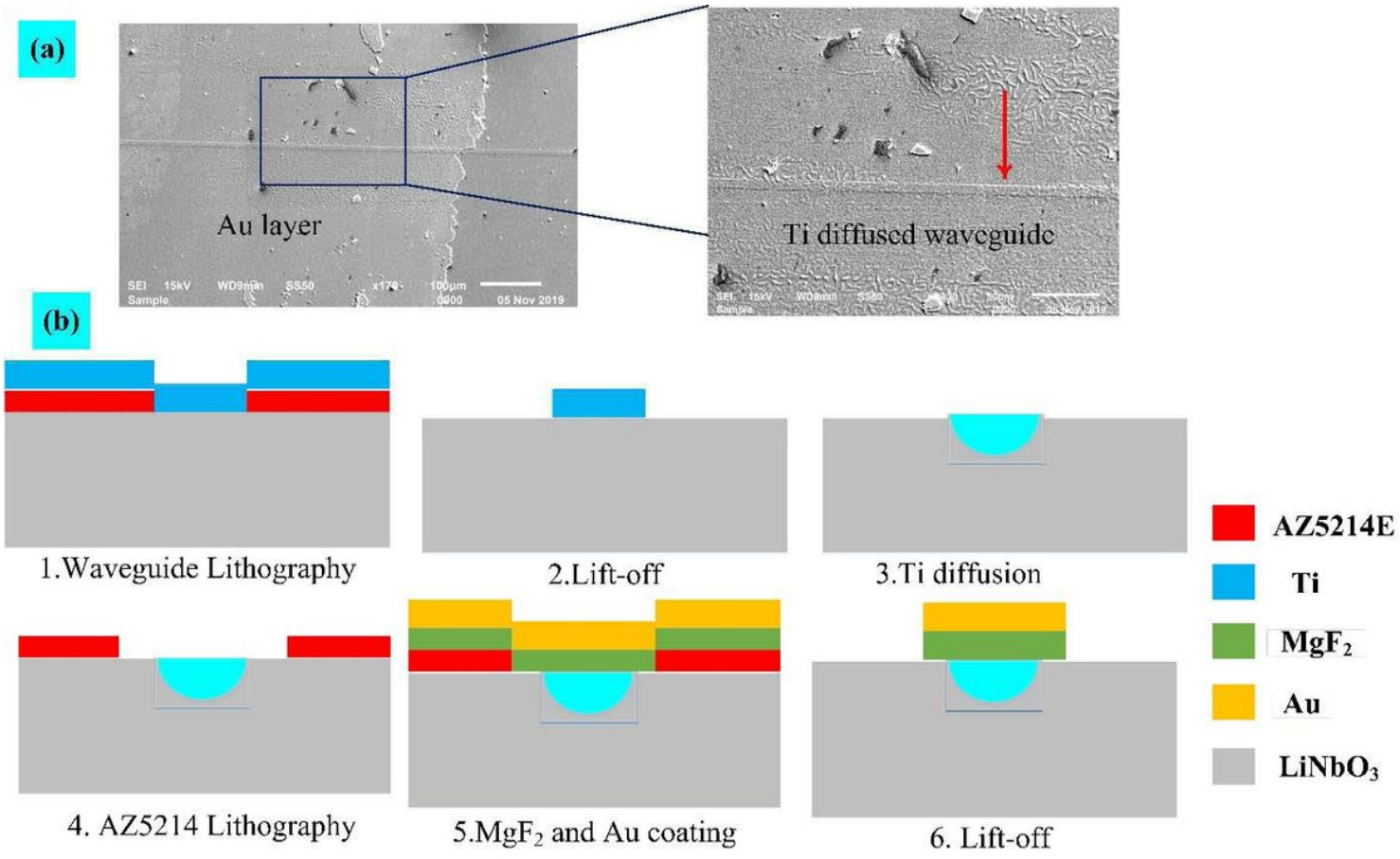

Figure 8

(a) SEM image of the fabricated plasmonic polarizer on a 8μm-width Ti: LiNbO3 channel waveguide. MgF2 layer of 5nm thickness is not clear.(b) The schematic diagram of the polarizer fabrication process

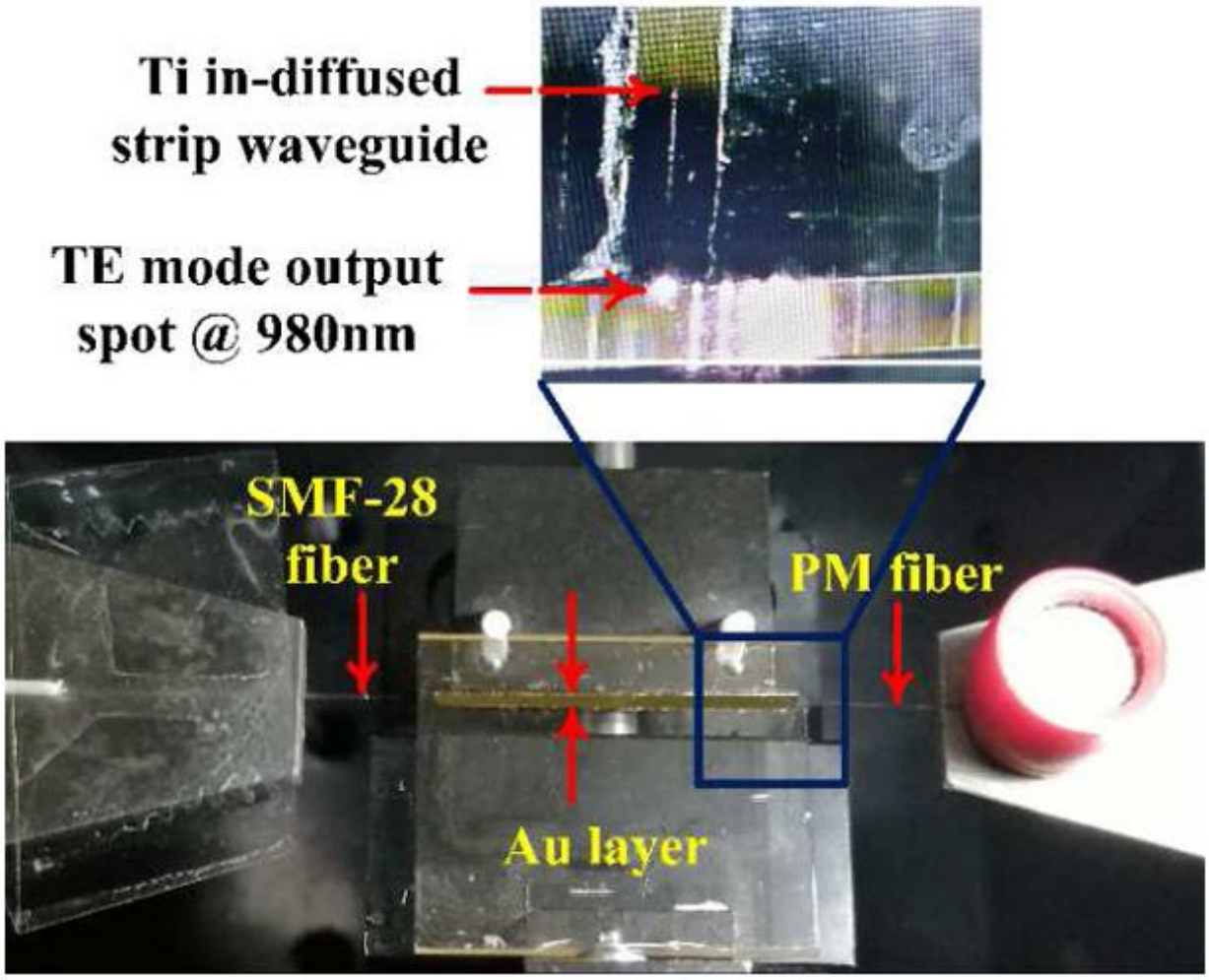

Figure 9

Coupling setup for characterization of the plasmonic polarizer.

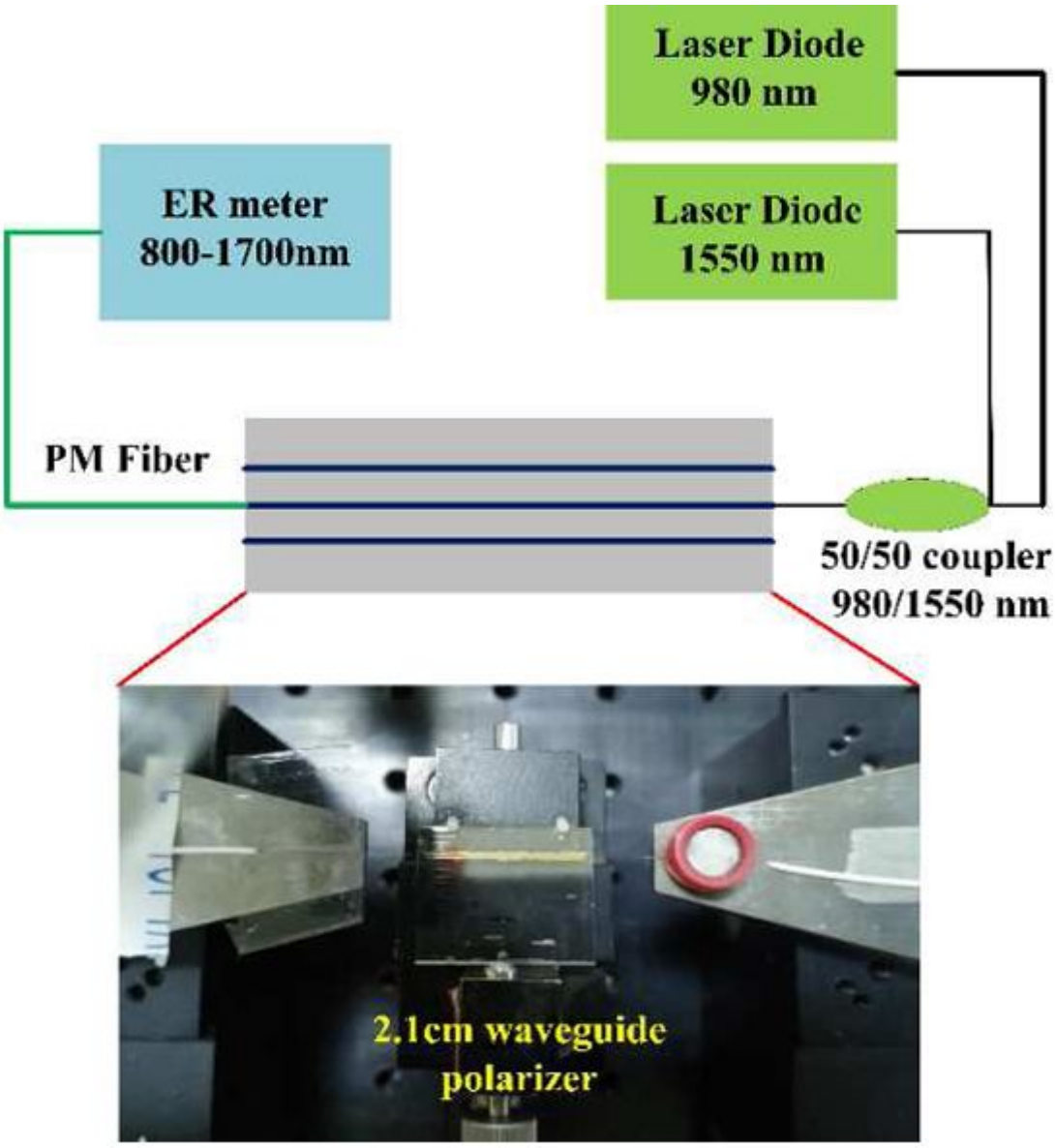

Figure 10

Characterization setup of the plasmonic polarizer.